IEEE Photonics Journal
An IEEE Photonics Society Publication

Open Access

Experimental Demonstration of RGB LED-Based Optical Camera Communications

Volume 7, Number 5, October 2015

Pengfei Luo
Min Zhang
Zabih Ghassemlooy
Hoa Le Minh
Hsin-Mu Tsai
Xuan Tang
Lih Chieh Png
Dahai Han

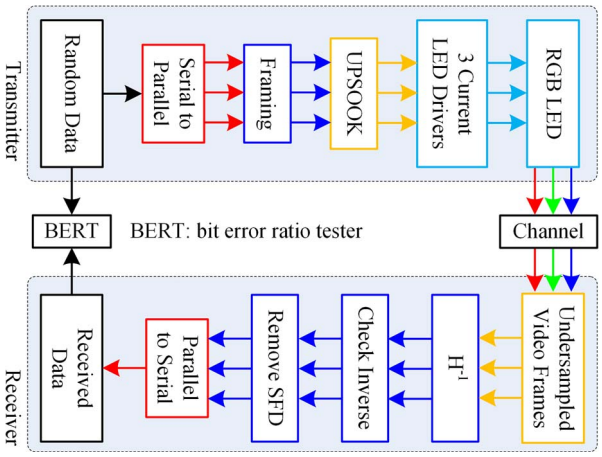

DOI: 10.1109/JPHOT.2015.2486680
1943-0655 © 2015 IEEE

Experimental Demonstration of RGB LED-Based Optical Camera Communications

Pengfei Luo,[1] Min Zhang,[2] Zabih Ghassemlooy,[1] Hoa Le Minh,[1] Hsin-Mu Tsai,[3] Xuan Tang,[4] Lih Chieh Png,[5] and Dahai Han[2]

[1]Optical Communications Research Group, NCRLab, Faculty of Engineering and Environment, Northumbria University, Newcastle upon Tyne NE1 8ST, U.K.
[2]State Key Laboratory of Information Photonics and Optical Communications, Beijing University of Posts and Telecommunications, Beijing 100876, China
[3]Department of Computer Science and Information Engineering, National Taiwan University,Taipei 106, Taiwan
[4]Fujian Institute of Research on the Structure of Matter, Chinese Academy of Sciences, Fuzhou 350002, China
[5]Division of Engineering Product Development, Singapore University of Technology and Design, Singapore 487372

DOI: 10.1109/JPHOT.2015.2486680

Manuscript received July 30, 2015; revised September 24, 2015; accepted September 28, 2015. Date of publication October 5, 2015; date of current version October 13, 2015. This work was supported by the EU cLINK project Grant 372242-1-2012-1-UK-ERA, the EU Cost Action IC 1101, the National Science Foundation of China Project 61471052, the Doctoral Scientific Fund of the Ministry of Education of China under Grant 20120005110010, the Fund of the State Key Laboratory of Information Photonics and Optical Communications (BUPT), and the Royal Society Newton International Exchanges (NI140188) between the U.K. and China. Corresponding author: P. Luo (e-mail: oliver.luo@northumbria.ac.uk).

Abstract: Red, green, and blue (RGB) light-emitting diodes (LEDs) are widely used in everyday illumination, particularly where color-changing lighting is required. On the other hand, digital cameras with color filter arrays over image sensors have been also extensively integrated in smart devices. Therefore, optical camera communications (OCC) using RGB LEDs and color cameras is a promising candidate for cost-effective parallel visible light communications (VLC). In this paper, a single RGB LED-based OCC system utilizing a combination of undersampled phase-shift on–off keying (UPSOOK), wavelength-division multiplexing (WDM), and multiple-input–multiple-output (MIMO) techniques is designed, which offers higher space efficiency (3 bits/Hz/LED), long-distance, and nonflickering VLC data transmission. A proof-of-concept test bed is developed to assess the bit-error-rate performance of the proposed OCC system. The experimental results show that the proposed system using a single commercially available RGB LED and a standard 50-frame/s camera is able to achieve a data rate of 150 bits/s over a range of up to 60 m.

Index Terms: Optical camera communication (OCC), visible light communications (VLC), non-flickering communication, red, green, and blue (RGB) light-emitting diode (LED), undersampled phase shift on-off keying (UPSOOK), wavelength division multiplexing (WDM), multiple-input-multiple-output (MIMO).

1. Introduction

Recently, RGB LEDs have been widely used in daily life especially in places where color-changing lighting is required, e.g., homes, shopping centers, and decorations, etc. One example of the color-changing light fixture is the Philips mood lighting system known as the “Hue,” which enables light tuning in terms of tone, contrast, and color spectrum to create ideal lighting conditions by using

smart devices such as smartphones or tablets [1]. Such lighting sources offer triple functionalities of illumination, data communication, and localization in an indoor environment [2]. Recently, cameras with a color filter array over an image sensor (IS) have also become very common in smart devices, which opens up valuable opportunities to use RGB LEDs as transmitters and built-in cameras on smart devices as receivers. This is known as optical camera communications (OCC) [3].

Unlike photodiode (PD)-based VLC systems [4], an OCC system uses a lens and a color IS to capture incident light signals in a sequence of video frames. Therefore, OCC systems possess a unique characteristic, which is the dual ability to separate light signals according to wavelengths and different directions of projection. This makes it possible for OCC to support wavelength division multiplexing (WDM) and imaging multiple-input-multiple-output (MIMO) techniques. This advantage could be effectively explored to demonstrate the potential capabilities of OCC systems for data transmission in a multitude of applications.

In general, for establishing a non-flickering VLC link, the frequency of the transmitted signal must be higher than the critical flicker frequency (CFF) of the human eye f_{max_eye} (~100 Hz [5]). However, for most commercial cameras, including both the built-in camera of commercial smart devices and the digital single-lens reflex (DSLR) cameras, their frame rate is commonly no more than 60 frames/s [6], [7]. Therefore, these low-frame-rate (LFR) cameras are not fast enough to capture every symbol in a data stream with a data rate higher than f_{max_eye}.

In order to ensure non-flickering data transmission with a LFR camera, the rolling shutter (RS) effect [8] and undersampled modulation-based schemes [9] have been introduced to OCC systems. According to [10], RS-based cameras follow a row-by-row exposure process to shoot videos. Therefore, when a light that flickers at a frequency with the same order of magnitude as the inverse of the shutter speed [11] is captured by a RS camera, a layer of dark and bright stripes superimposed on the normal image will be recorded; consequently, the original data can be extracted from these dark and bright stripes [8]. In contrast, in undersampled intensity modulation (IM) based schemes, the camera pointing at the transmitting LEDs will observe a series of states (on, off, etc.) representing the LED image rather the dark and bright stripes.

Although both methods are able to support non-flickering OCC, there are still some drawbacks that need addressing. In RS effect schemes, the entire or a large part of the IS is exposed to the illumination level, thus restricting the transmission span [12] as well as the spatial multiplexing capabilities of OCC systems [13]. In previously reported undersampled modulation schemes, each received LED state only represents a single bit [9] or half a bit of information (two LED states are required to recover one bit of information) [14], which severely limits the total throughput in single LED based transmission systems.

In order to demonstrate an OCC system that is able to work over long distances (e.g., outdoor car-to-car communication using OCC) with high spectral efficiency, we propose an improved RGB LED-based OCC system that increases the spectral efficiency from 0.5 bit/Hz/LED of undersampled frequency shift on and off keying (UFSOOK) to 3 bits/Hz/LED, thus making it possible to transmit higher data rates by using just a single RGB LED and a LFR camera. The main contribution of this paper is to demonstrate a non-flickering, long range, and parallel VLC system based on the combination of undersampled phase shift OOK (UPSOOK), WDM, and MIMO techniques with a dedicated framing structure and employing a single RGB LED light source and a LFR camera. Moreover, in this paper, we have carried out the overall analysis and performance evaluation of the proposed system.

The rest of this paper is organized as follows: The operation principle of each technique and the system design are detailed in Section 2. The performance evaluation of the proposed system is given in Section 3. Finally conclusions are drawn in Section 4.

2. Principles of Operation and System Design

In this section the operating principles of UPSOOK and an RGB LED-based WDM OCC system based on a 3×3 MIMO are described in detail. The system design of the proposed OCC system is also presented.

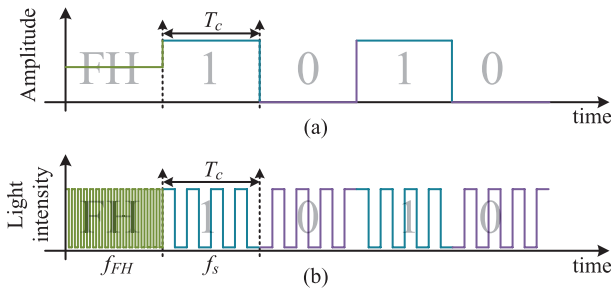

Fig. 1. (a) Original base band data and (b) UPSOOK modulated signal ($T_c = 20$ ms, $f_s = 200$ Hz, and $f_{FH} = 10$ kHz).

2.1. UPSOOK

The process of a bandpass-filtered signal being sampled with a sampling frequency lower than the upper cut-off frequency and then successfully reconstructed is known as undersampling [15]. It can be used to support non-flickering OCC with a LFR camera. UPSOOK modulation (1 bit/Hz/LED) was first proposed in [9], which employed phase shift keying (PSK) to modulate a square wave carrier with a frequency f_s higher than $f_{\text{max\_eye}}$ and lower than the inverse of the shutter speed, and used a LFR camera to undersample the original baseband data $\{a_n\}$.

The UPSOOK signal $s(t)$ can be expressed as

$$s(t) = \lceil \cos(2\pi f_s t + \theta_n) \rceil, \qquad 0 < t \leq T_c \tag{1}$$

where $\lceil \bullet \rceil$ denotes a square wave, T_c is the duration of $\{a_n\}$, and θ_n is the carriers phase, which is defined as

$$\theta_n = \begin{cases} 0^\circ, & a_n = 1 \\ 180^\circ, & a_n = 0. \end{cases} \tag{2}$$

In order to frequency-synchronize the transmitter (Tx) and the camera, we set $T_c = 1/f_c$, and $f_s = m \times f_c$, where f_c is the frame rate of the camera, and m is an integer. Hence, during each T_c, there are exactly m pulses transmitted via an LED. Fig. 1 presents an example of $\{a_n\}$ and the corresponding UPSOOK modulated signal. As shown in Fig. 1(a) the 1st bit is labeled as the frame header (FH), which is used to let the receiver (Rx) determine the beginning of each data frame, followed by 4-bit: [1, 0, 1, 0]. It is clear from Fig. 1(b) that the modulated FH is a 50% duty cycle square wave with a frequency of f_{FH}, which is much higher than the CFF of the camera $f_{\text{max\_camera}}$ (according to our experimental result, $f_{\text{max\_camera}}$ is the same order of magnitude as the inverse of the shutter speed).

Generally, when a camera is used to record video signals, its IS captures f_c frames per second with each video frame being exposed to t_e second [16], as illustrated in Fig. 2. Thus, the camera can be considered as an integrate-and-dump filter with an integration time of t_e and a sampling frequency of f_c. Therefore, a camera pointing at an LED will capture three states: i) an ON state when LED is on at all time with a constant transmit optical power; ii) a HALF ON (HO) state when the LED is intensity modulated with 50% duty cycle pulse stream having a pulse duration $< t_e$; and iii) an OFF state when the LED is switched off during t_e.

Accordingly, when an LED that is emitting the above-mentioned UPSOOK signals [see Fig. 1(b)] is recorded by a camera, there will be two possible scenarios on the captured image depending on the sampling phase as shown in Fig. 3(a). In the 1st scenario, the sampled light levels, shown above the red dotted arrows, are the same as the transmitted signal as in Fig. 1(a): ON for bit 1, OFF for bit 0, and HO for FH. In the 2nd case, the sampled LED states, shown below the blue solid arrows, are not the same as the transmitted signal. However, the correct values can be obtained by simply inverting the sampled states. Fig. 3(b) illustrates the three recorded LED intensity states. Although the phase uncertainty between the Tx and Rx

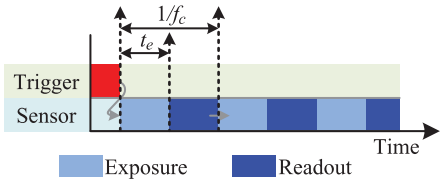

Fig. 2. Basic video capturing process [16].

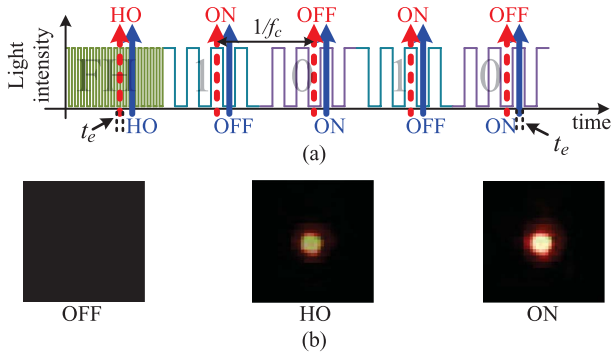

Fig. 3. (a) Two possible undersampled results ($f_c = 50$ Hz) for the same transmitted signal and (b) three possible sampled LED states.

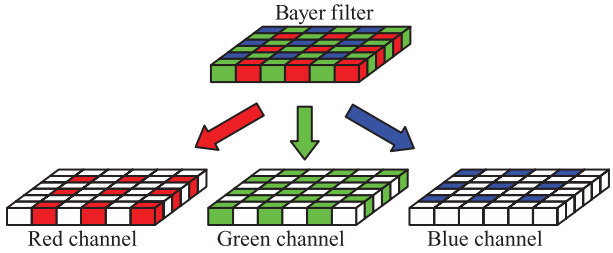

Fig. 4. Bayer RGB filter pattern [17].

might result in errors when assigning bits as 1 or 0, the FH will not be affected since it will always be captured as the HO state, see Fig. 3(a).

To avoid this uncertainty and to obtain the channel matrix (see Section 2.3), a framing strategy, which allows the receiver to detect and correct the phase uncertainty caused error, as well as demultiplexing the MIMO signal, is proposed in detail in Section 2.4.

2.2. WDM

As mentioned above, the color camera has the ability to separate light signals according to third wavelengths, which is realized by a color filter array on a square grid of pixels of an IS. The most common type of color filter array is called a "Bayer array" [16], with 50%, 25%, and 25% of green, red, and blue regions, respectively; see Fig. 4, which allows separation of light according to the wavelength. On exposing the filter to the incoming light containing different colors, each small filter will permit only particular colors to pass through. This feature opens an opportunity to establish a WDM link by sending three parallel data streams via the RGB LEDs.

However, due to the wide optical bandwidth of R, G, B color filters (see Fig. 5(a), which shows the measured intensity profiles of the RGB channels for the Nikon D5000 DSLRs IS [18]), there will be a color spectrum overlap between each pair of channels. Additionally, RGB LEDs normally have a wide intensity spectral profile (see Fig. 5(b), which leads to inter-channel

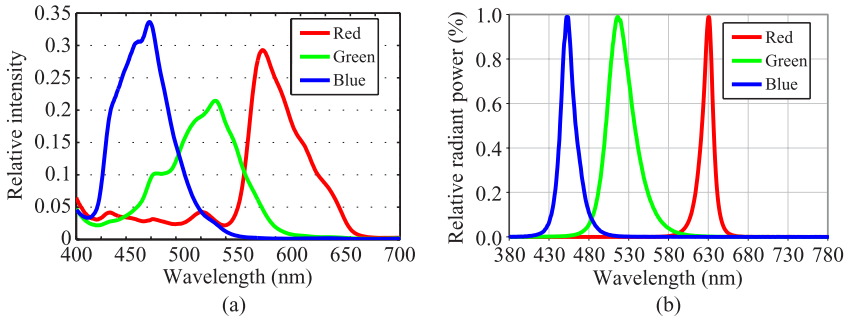

Fig. 5. Relative intensity profiles for (a) a Nikon D5000 DSLR optics and sensors [18] and (b) Cree XLamp MC-E RGB LED [20].

interference (ICI) at the Rx). Therefore, it may not be possible to realize three independent channels by simply employing RGB LEDs and a color camera. In order to reduce the inter-channel cross-talk (ICCT), the best option would be to adopt the parallel transmission scheme as in MIMO systems [19]; this will be introduced in the following subsection.

2.3. MIMO

As outlined above, the overlap of the RGB camera spectra response and the broad spectral range of the RGB LEDs will lead to ICCT. For example, when capturing a green light, the camera's green channel will receive the highest optical power. However, some of the power (i.e., cross-talk) will also appear at both the red and blue channels, which depends on the wavelength of the incident light and the spectral characteristics of RGB filters. Therefore, to ensure that these three parallel channels do not interfere with each other, a MIMO technique, which works on the color-based concept but not spacing, is adopted that enables the Rx to entirely separate the parallel RGB signals.

In RGB LED based OCC systems, the line-of-sight (LOS) DC channel gain for each RGB LED—RGB Rx pair is described by the channel matrix H given by [19]

$$H = \begin{bmatrix} h_{\mathrm{RR}} & h_{RG} & h_{\mathrm{RB}} \\ h_{\mathrm{GR}} & h_{\mathrm{GG}} & h_{\mathrm{GB}} \\ h_{\mathrm{BR}} & h_{\mathrm{BG}} & h_{\mathrm{BB}} \end{bmatrix} \tag{3}$$

where, for example, h_{RR} is the channel gain from the red LED to the red channel, and h_{RG} is the channel gain from the red LED to the green channel, and so on.

Hence, the optical power from RGB channels captured by a digital camera is given by [21]

$$Y = HX + N \tag{4}$$

where Y and X are the received and transmitted optical power vectors, respectively, and N is the noise power vector, which are defined as

$$\begin{cases} Y = [\, y_R \quad y_G \quad y_B \,]^{\mathrm{T}} \\ X = [\, x_R \quad x_G \quad x_B \,]^{\mathrm{T}} \\ N = [\, n_R \quad n_G \quad n_B \,]^{\mathrm{T}}. \end{cases} \tag{5}$$

Following the approach adopted in [19] the estimated transmitted signal X_{est} is given by

$$X_{est} = H^{-1} Y. \tag{6}$$

Fig. 6 illustrates a schematic diagram of the RGB filter based MIMO system. In order to obtain the channel matrix H, a parallel pilot signal (PPS) should be transmitted to the camera prior to transmission of the information data. The simplest PPS could be based on the identity matrix,

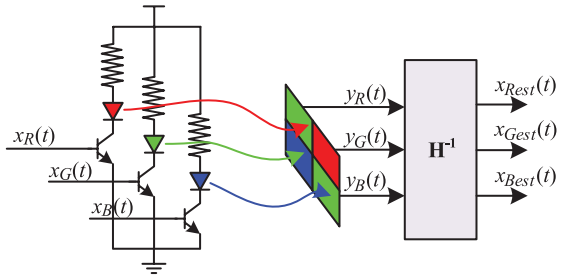

Fig. 6. Schematic diagram of the RGB filter-based MIMO system.

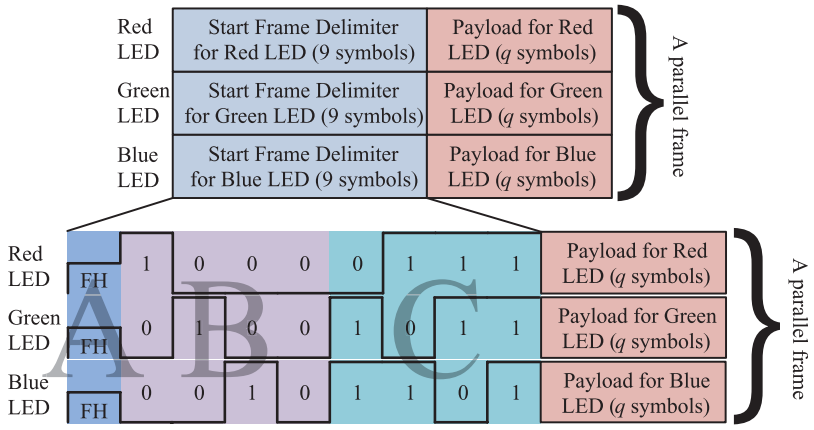

Fig. 7. Parallel data frame structure.

which means the red, green, and blue LEDs are switched on in turn; thus, each channel gain can be obtained sequentially. Furthermore, MIMO demultiplexing can be performed with the received H matrix.

2.4. Framing Structure

In order to detect and correct the error caused by non-synchronized phase (see Section 2.1), and obtain the 3×3 H matrix for the MIMO demultiplexing process (see Sections 2.2 and 2.3), a data frame structure is adopted for the RGB LED based OCC system. Since the proposed system has three parallel channels, the framing procedure must process three channels synchronously. Fig. 7 demonstrates the proposed frame structure, which is composed of two fragments: i) the start-frame delimiter (SFD) with nine data symbols and ii) the payload with q data symbols, where q is an arbitrary number; see the upper section of Fig. 7.

The lower section of Fig. 7 demonstrates the detailed structure of the SFD, which is composed of three parts labeled as A, B, and C. Part A is especially designed to indicate the start of a data frame, see Fig. 7, and has three FH symbols in parallel. Therefore when the camera captures the UPSOOK modulated signal of this part, the recorded RGB LEDs will be in HO states [see the first symbol in Fig. 3(a)]. Part B is designed to obtain the H matrix and to check the phase error. The first three parallel symbols are the identity matrix for obtaining the 3×3 H matrix, and the fourth symbol is a parallel zero that can be used to indicate the phase error at Rx. However, because of the phase uncertainty [see Fig. 3(a)], part C, which is the complement version of part B, is required to ensure that the H matrix can still be captured in the presence of the phase error.

Fig. 8 presents two captured parallel RGB LED states without ICI. Note that, due to the interference from the neighboring channels, the real captured LED states will not be the same as in Fig. 8 (see Fig. 13 for experimentally measured parallel waveforms).

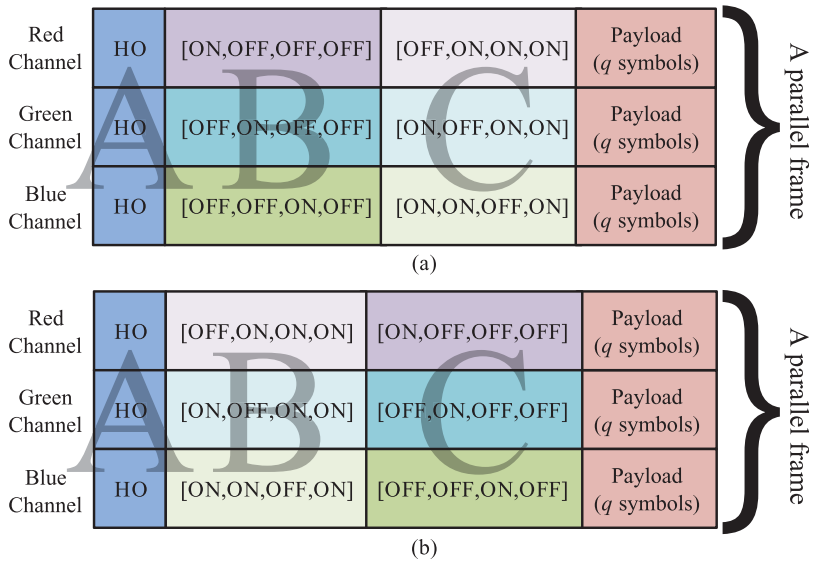

Fig. 8. Two possible received data frames without ICI. (a) No need to do error correction and (b) error correction is needed.

It is clear that the first column of Fig. 8(a) and (b) is in the HO state, which indicates the start of SFD. When the fifth and ninth columns are in the OFF and ON states, respectively, this indicates that there are no phase errors [see Fig. 8(a)]. Therefore, the H matrix can be obtained from the second to fourth parallel symbols of the SFD, and the estimated transmitted payload can be calculated using (6) (see Appendix for detail). However, if the 5th and 9th columns are the opposites of those at the corresponding positions of Fig. 8(a) [i.e., Fig. 8(b)], then the H matrix can be determined from the 6th–8th parallel symbols in part C. The inverse operation of each symbol (changing ON to OFF, OFF to ON) will be required in order for the entire received frame to correct the phase-induced error after de-multiplexing of mixed signals with (6).

2.5. Experimental Setup

An experimental test bed was put together to measure the performance of the proposed RGB LED based OCC system as shown in Fig. 9. The Tx consisted of a quasi-random data source, serial to parallel (S/P) convertor, framing procedure, UPSOOK, 3 current LED drivers, and an RGB LED. In the experiment, the first four blocks on Tx were realized in MATLAB and then applied to an arbitrary waveform generator (AWG) for IM of LEDs. Three LED current drivers [NU511 from Numen Technology, Inc. [22] Fig. 10(a)] were used to control the output light of the RGB LEDs [Cree XLamp MC-E RGB LED lamp Fig. 10(b)]. At the Rx side, the received RGB lights were undersampled and captured using a DSLR camera (Canon EOS 700D kit, EF-S 18–55 mm IS STM lens). The parallel signals were then passed through the inverse H matrix (H^{-1}), "check inverse" module, "remove SFD" module, and parallel-to-serial (P/S) module to recover the original data. All signal processing was performed off-line in MATLAB.

3. Performance Evaluation

A proof-of-concept RGB LED-based OCC test bed, pictured in Fig. 11, was built to make field measurements in an underground parking space. At the Tx side, three parallel UPSOOK data frames generated by MATLAB were repeatedly sent via the RGB LED. At the Rx side, a Canon 700D (placed at distances d within the range of 15 m–75 m from the Tx) was used to capture two minutes video of the RGB LED lamp. MATLAB was used for processing the captured video signal to obtain the RGB values of all pixels constituting the LED image in each video frame, and to calculate the sum of RGB values of the red, green, and blue channels. In the experiments,

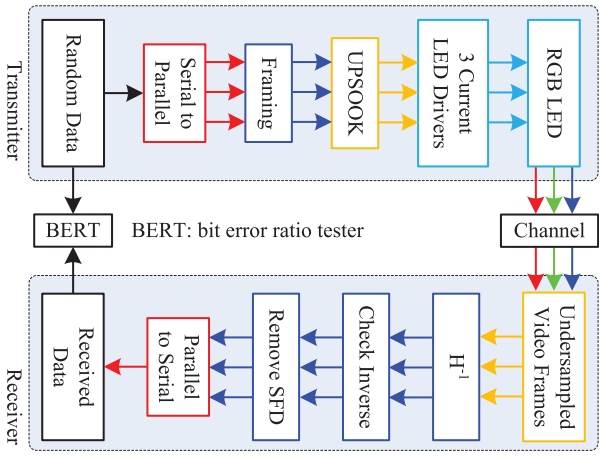

Fig. 9. Schematic block diagram of the experimental test bed of the OCC system.

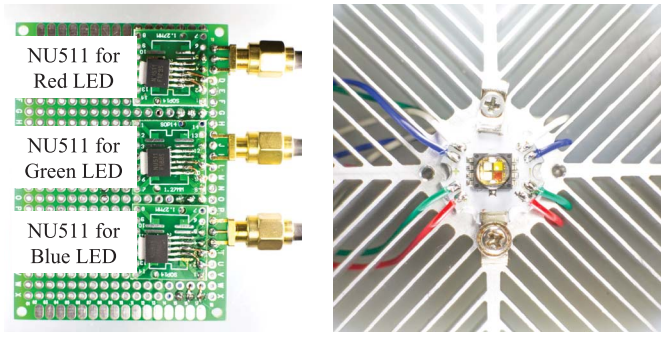

Fig. 10. Images of (a) three constant current LED drivers and (b) Cree XLamp MC-E RGB LED lamp on a heat sink.

q was set to 500, while f_c and f_s were set to 50 Hz and 250 Hz, respectively. All other key parameters are listed in Table 1.

In order to evaluate the performance of the OCC test bed, we carried out a number of experiments for a range of transmission spans d. For each d, we repeated the experiment for six times and captured around 36000 video frames. This gave us a total number of received raw bits from the three parallel channels of almost 1.08×10^5.

Fig. 12(a) illustrates the normalized captured average RGB value of the LED image against the transmission distance. The figure illustrates the joint effect of gamma-correction [23] and d on the average received optical power, which drops rapidly for $d \leq 40$ m. However, when $d > 40$ m, the rate of decrease of the received optical power slows down, especially when $d > 60$ m. This is because the irradiance varies with distance according to the inverse square law [24]. The measured bit error rate (BER) performance is shown in Fig. 12(b). Note that we only sent $\sim 1.08 \times 10^5$ bits for each distance. For the measured BER of zero, it was set to 1×10^{-5}. As shown in Fig. 12(b) at a BER of 1×10^{-5} the data rate is 150 bits/s for d up to at least 25 m. For d doubling (e.g., from 30 m to 60 m) the BER increases two orders of magnitude. At d of 60 m the BER is 3.1×10^{-3}, which is less than the FEC limit of 3.8×10^{-3} [25].

Fig. 13 shows the captured RGB waveforms for four values of d (20 m, 35 m, 50 m, and 65 m). Although there is cross-talk between the channels, we can still easily determine the HO state parallel symbol, which is the unique symbol among all received symbols. As stated in Section 2.4,

Fig. 11. RGB LED-based OCC experimental setup.

TABLE 1
Key parameters of experiment

Parameter	Value
Average driver current for each channel	350 mA
FH frequency	10 kHz
Test distance d	15 m - 75 m
Shutter speed	$1/4000$ s
Focal length (FL)	55 mm
Camera aperture	$f/36$
Camera ISO	100
Video resolution	960×720
Half-angle of condenser cup	$35°$

this symbol is known as FH, which indicates the start of a data frame. Therefore we are able to check phase error and obtain the H^{-1} matrix from the following 8 symbols. With reference to Figs. 7 and 8, it is clear that there are no phase errors in Fig. 13(a) and (c); however, phase errors are present in Fig. 13(b) and (d). Note that the drop in the amplitude of the waveforms is due to the increase in the transmission distance.

Although the total raw data rate used was 150 bits/s, higher data rates could be achieved by increasing the number of RGB LEDs and using the imaging MIMO technology [26], which would be ideal for car to car communications.

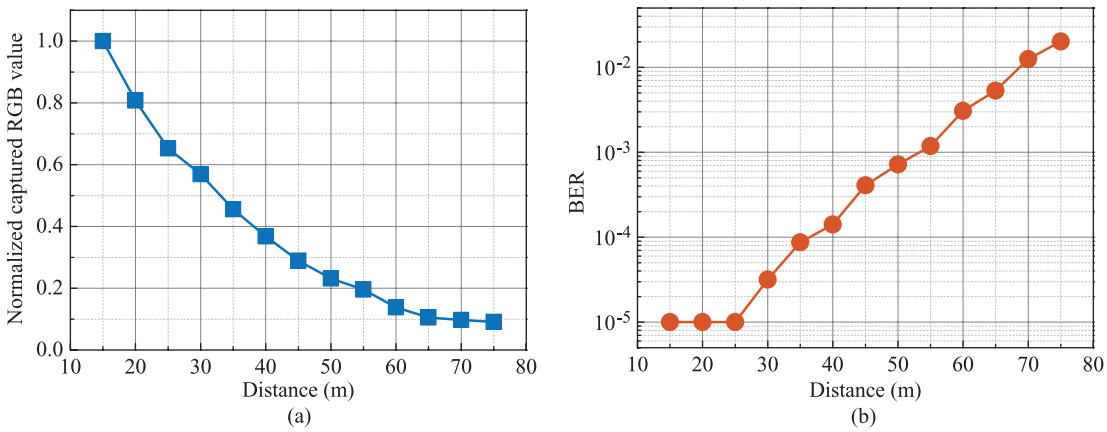

Fig. 12. (a) Relative sum of captured RGB values from the LED image and (b) BER performance of the RGB LED-based OCC test bed under different communication distances in an underground parking garage.

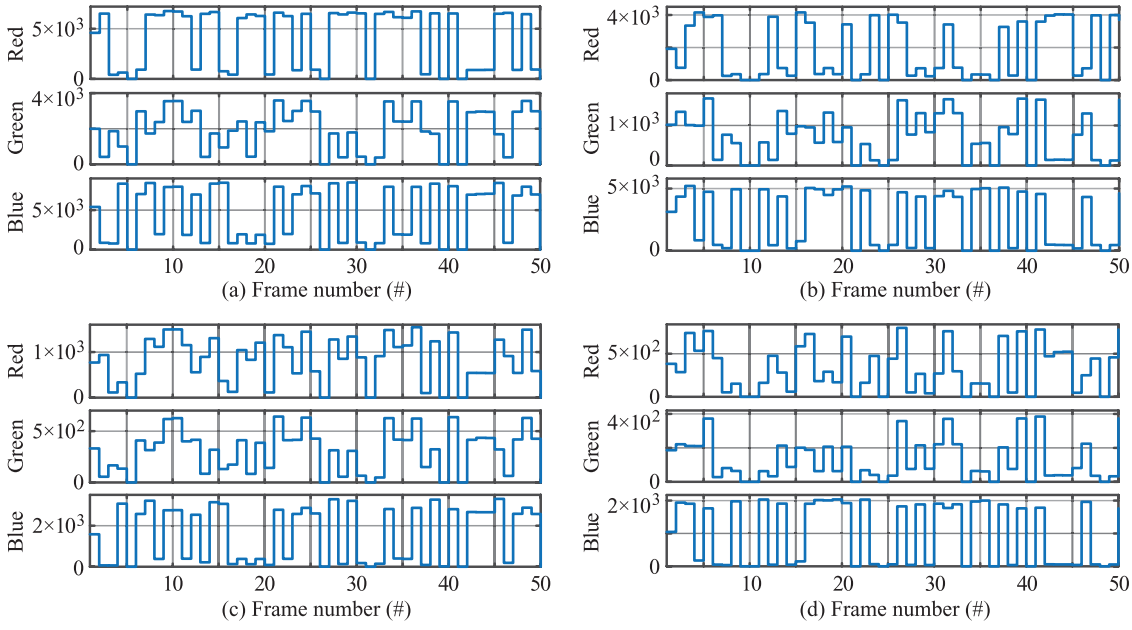

Fig. 13. Received RGB waveforms at distances of (a) 20 m, (b) 35 m, (c) 50 m, and (d) 65 m. (y-axis is the sum of RGB values from the red, green, and blue channel of the captured LED video frames).

4. Conclusion

In this work, we demonstrated an experimental RGB LED-based WDM OCC system by employing a combination of UPSOOK, WDM, and MIMO technologies to overcome the problem of light flickering and inter-channel-interference. A framing structure was proposed and designed to obtain the H matrix for demultiplexing the mixed RGB signals and checking the receiver phase error. The experimental results demonstrated that the developed test bed is able to achieve a raw data rate of 150 bits/s by using one RGB LED and a 50 frames/s camera over a transmission span up to 60 m. However, higher data rates over longer link spans could be achieved by using a larger number of high power RGB LEDs.

Future work on this topic will consider i) employing video tracking technology, ii) re-designing the frame structure in order to obtain a higher quality H^{-1} matrix for more accurate estimation of

	A	B			C				D					
Red	FH	1	0	0	0	1	1	1	1	1	0	1	1	0
Green	FH	0	1	0	0	1	0	1	1	1	1	0	0	0
Blue	FH	0	0	1	0	1	1	0	1	1	0	1	0	1	1

(a)

	A	B			C				D					
Red	4593	6504	415	636	0	920	6412	6349	6762	6713	6246	928	6483	6665	765
Green	1998	417	1864	1000	0	2979	1734	2378	3552	3557	2385	3008	419	1736	949
Blue	5403	866	779	8339	0	7027	8422	1955	7921	7959	1858	6971	841	8350	8458

(b)

Fig. 14. First 15 data columns of a data frame from (a) transmitter and (b) receiver side.

the data, and iii) increasing the number of RGB LEDs to increase the throughput with imaging MIMO technology.

Appendix

This section gives an example of how we estimate the transmitted data.

Fig. 14 demonstrates the first 15 data columns of a data frame from both Tx and Rx [received RGB values; see Fig. 13(a)]. It can be observed from the figure that 15 columns are divided into 4 parts (from A to D) in according to Fig. 8, where D is the payload. By comparing Fig. 14(a) with Fig. 14(b), we conclude that the received results are without the phase error, therefore the H matrix is obtained from the first 3 columns of part B. Thus, we have

$$H = \begin{bmatrix} 6504 & 415 & 636 \\ 417 & 1864 & 1000 \\ 866 & 779 & 8339 \end{bmatrix}. \tag{7}$$

Consequently, the transmitted signal can be estimated by (6), which is given as

$$X_{est} = \begin{bmatrix} 0.88 & 0.89 & -0.01 & 1.00 & 0.92 & 0.02 \\ 1.31 & 1.06 & 1.23 & 0.00 & 0.25 & -0.04 \\ 0.74 & 0.03 & 0.72 & 0.00 & 0.88 & 1.02 \end{bmatrix}. \tag{8}$$

Once a threshold level of 0.5 is applied to (8), the estimated data then are given as

$$X_{est} = \begin{bmatrix} 1 & 1 & 0 & 1 & 1 & 0 \\ 1 & 1 & 1 & 0 & 0 & 0 \\ 1 & 0 & 1 & 0 & 1 & 1 \end{bmatrix}. \tag{9}$$

This is the same as part D of Fig. 14(a), indicating that the estimated data are the same as the transmitted data.

References

[1] M. R. Luo, Z. Fan, Z. Qiyan, L. Xiaoyu, and W. Binyu, "The impact of led on human visual experience," in *Proc. IEEE 10th China SSL*, 2013, pp. 280–283.

[2] Z. Ghassemlooy, W. Popoola, and S. Rajbhandari, *Optical Wireless Communications: System and Channel Modelling With MATLAB*. Boca Raton, FL, USA: CRC, 2012.

[3] I. Takai *et al.*, "Optical vehicle-to-vehicle communication system using LED transmitter and camera receiver," *IEEE Photon. J.*, vol. 6, no. 5, pp. 1–14, Oct. 2014.

[4] L. Grobe *et al.*, "High-speed visible light communication systems," *IEEE Commun. Mag.*, vol. 51, no. 12, pp. 60–66, Dec. 2013.

[5] C. S. Herrmann, "Human EEG responses to 1–100 Hz flicker: resonance phenomena in visual cortex and their potential correlation to cognitive phenomena," *Exp. Brain Res.*, vol. 137, no. 3/4, pp. 346–353, Apr. 2001.

[6] T. Hao, R. Zhou, and G. Xing, "COBRA: Color barcode streaming for smartphone systems," in *Proc. 10th Int. Conf. Mobile Syst., Appl., Serv.*, 2012, pp. 85–98.

[7] M. Parker and S. Dhanani, "Digital video processing for engineers: A foundation for embedded systems design," in *Introduction to Video Processing*. Oxford, U.K.: Newnes, 2013.
[8] H.-M. Tsai, H.-M. Lin, and H.-Y. Lee, "Demo: Rollinglight-universal camera communications for single LED," in *Proc. 20th Annu. Int. Conf. Mobile Comput. Netw.*, 2014, pp. 317–320.
[9] P. Luo, Z. Ghassemlooy, H. L. Minh, X. Tang, and H.-M. Tsai, "Undersampled phase shift ON-OFF keying for camera communication," in *Proc. 6th Int. Conf. WCSP*, 2014, pp. 1–6.
[10] M. Meingast, C. Geyer, and S. Sastry, "Geometric models of rolling-shutter cameras," in *Proc. Omnidirectional Vis., Camera Netw. Non-classical Cameras*, 2005, pp. 12–19.
[11] N. Rajagopal, P. Lazik, and A. Rowe, "Visual light landmarks for mobile devices," in *Proc. 13th Int. Symp. Inf. Process. Sensor Netw.*, 2014, pp. 249–260.
[12] P. Ji, H.-M. Tsai, C. Wang, and F. Liu, "Vehicular visible light communications with LED taillight and rolling shutter camera," in *Proc. IEEE Veh. Technol. Conf.*, Spring 2014, pp. 1–6.
[13] C. Danakis, M. Afgani, G. Povey, I. Underwood, and H. Haas, "Using a CMOS camera sensor for visible light communication," in *Proc. IEEE GC Wkshops*, 2012, pp. 1244–1248.
[14] R. D. Roberts, "Undersampled frequency shift ON-OFF keying (UFSOOK) for camera communications (CamCom)," in *Proc. IEEE 22nd WOCC*, 2013, pp. 645–648.
[15] W. Kester, "Mixed-signal and DSP design techniques," in *Sampled Data Systems*. Oxford, U.K.: Newnes, 2003.
[16] Thorlabs, "CCD and CMOS cameras operation manual and SDK," 2015.
[17] P. Cheremkhin, V. Lesnichii, and N. Petrov, "Use of spectral characteristics of DSLR cameras with Bayer filter sensors," in *Proc. J. Phys.: Conf. Series*, vol. 536, 2014, Art. ID. 012021.
[18] D. L. Bongiorno, M. Bryson, D. G. Dansereau, and S. B. Williams, "Spectral characterization of COTS RGB cameras using a linear variable edge filter," in *Proc. IS&T/SPIE Electron. Imag. Int. Soc. Opt. Photon.*, 2013, Art. ID. 86600N.
[19] A. Burton, H. L. Minh, Z. Ghassemlooy, E. Bentley, and C. Botella, "Experimental demonstration of 50-Mb/s visible light communications using 4×4 MIMO," *IEEE Photon. Technol. Lett.*, vol. 26, no. 9, pp. 945–948, May 2014.
[20] "Cree XLamp MC-E LED data sheet," Cree Inc., Durham, NC, USA, 2015.
[21] P. A. Haigh *et al.*, "A MIMO-ANN system for increasing data rates in organic visible light communications systems," in *Proc. IEEE ICC*, 2013, pp. 5322–5327.
[22] "NU511 - 1.2A single channel LED driver," N. Tech., Zhubei, Taiwan, 2015.
[23] S. Wright, "Digital compositing for film and video," *Gamma*. New York, NY, USA: Taylor & Francis, 2013.
[24] A. Ryer, "Light measurement handbook," Int. Light Inc. Peabody, MA, USA, 1998.
[25] "G.975.1, Forward error correction for high bit-rate DWDM submarine systems," Int. Telecommun. Union (ITU-T), Geneva, Switzerland, 2004.
[26] S. H. Chen and C. W. Chow, "Color-filter-free spatial visible light communication using RGB-LED and mobile-phone camera," *Opt. Exp.*, vol. 22, no. 25, pp. 30 713–30 718, Dec. 2014.